is forbidden to first order,[42] it is possible that higher order effects, combined with coupling to higher energy charge-transfer states, may be sufficient to produce such a displacement.

Conclusions

The overall energies, polarization behavior, vibrational fine structure, and temperature dependence of the bands observed in the electronic spectra of the planar $CuCl_4^{2-}$ ions in $(metH)_2CuCl_4$ and $(creat)_2CuCl_4$ may be explained reasonably well within the normal theoretical framework of vibronic coupling and ligand field theory described in previous publications. As with other similar complexes, the $^2A_{1g}(z^2) \leftarrow {}^2B_{1g}(x^2-y^2)$ transitions occur at unusually high energy, possibly due to configuration interaction between the metal $a_{1g}(d_{z^2})$ and $a_{1g}(4s)$ orbitals. Analysis of the vibrational structure observed on the transitions to the $^2B_{2g}(xy)$ and $^2A_{1g}(z^2)$ excited states of $(metH)_2CuCl_4$ suggests a lengthening of each Cu–Cl bond of ~8 and ~11 pm, respectively, in good agreement with theoretical predictions.

An unusual aspect of the spectra not readily explicable by using current simple theories is the abnormally large red shift observed for the band maxima of each "d–d" transition on warming from 10 to 290 K. An attempt has been made to explain these shifts in terms of a temperature-dependent low-symmetry component to the ligand field, this being caused by the low-energy β_{2u} vibration, which carries the complex from a planar toward a distorted-tetrahedral geometry. However, it was found that in order to explain the band maxima shifts in this way, the energy of the β_{2u} mode would have to be about half of the estimate of ~60 cm^{-1} obtained from the analysis of the temperature dependence of the band intensities. The cause of this discrepancy is not clear.

Acknowledgment. The financial support of the Australian Research Grants Scheme is gratefully acknowledged. The Central Science Laboratory of the University of Tasmania is thanked for the loan of the cryostat used in the present work and Mark Riley is thanked for several useful discussions.

Registry No. $(metH)_2CuCl_4$, 72268-09-8; $(creat)_2CuCl_4$, 70602-46-9.

(41) Martin, D. S., Jr.; Tucker, M. A.; Kassman, A. J. *Inorg. Chem.* **1965**, *4*, 1682.

(42) We are concerned with the way in which the energy of an excited state ψ changes as the geometry alters from the equilibrium nuclear geometry of the ground state along a normal mode Q. This may be expressed as a power series:

$$\left\langle \psi \middle| \left(\frac{\partial H}{\partial Q}\right)_0 \middle| \psi \right\rangle Q + \left\langle \psi \middle| \left(\frac{\partial^2 H}{\partial Q^2}\right)_0 \middle| \psi \right\rangle Q^2 + \ldots$$

from which it follows that if ψ is nondegenerate, then Q must transform as α_{1g} for the linear term to be non-zero. Professor E. I. Solomon of Stanford University is thanked for pointing out this fact. However, it should be noted that this restriction does not apply to terms involving even powers: Q^2 etc.

(43) Deeth, R. J.; Hitchman, M. A.; Lehmann, G.; Sachs, H. *Inorg. Chem.* **1984**, *23*, 1310.

Contribution from the Departments of Chemistry, Texas A&M University, College Station, Texas 77843, and University of Delaware, Newark, Delaware 19716

Ligand Substitution Processes in Tetranuclear Carbonyl Clusters. 10. X-ray Structural Characterization of Products Resulting from Reactions of $Co_4(CO)_9(tripod)$, tripod = $HC(PPh_2)_3$, with Phosphine Ligands

Donald J. Darensbourg,*[1a] David J. Zalewski,[1a] Arnold L. Rheingold,*[1b] and Rebecca L. Durney[1b]

Received January 28, 1986

The solid-state geometry of $Co_4(CO)_8(PMe_3)$(tripod) (I), $Co_4(CO)_7$(dppm)(tripod) (II), and $Co_4(CO)_7(PMe_3)_2$(tripod) (III) were determined by single-crystal X-ray diffraction studies. I crystallizes in an orthorhombic cell *Pbca* with a = 16.864 (5) Å, b = 16.989 (3) Å, and c = 34.676 (9) Å with eight molecules per unit cell. II crystallizes in a monoclinic cell $P2_1/c$ with a = 12.001 (4) Å, b = 21.955 (10) Å, c = 25.329 (9) Å, and β = 99.40 (3)° with four molecules per unit cell. III crystallizes in an orthorhombic cell $Pca2_1$ with a = 24.831 (6) Å, b = 11.999 (2) Å, and c = 19.191 (4) Å with four molecules per unit cell. The structures were refined to the following values: I to R = 0.0626 and R_w = 0.0589, II to R = 0.0900 and R_w = 0.0910, and III to R = 0.0706 and R_w = 0.0663. The solid-state structures were used to substantiate the solution structural assignments based on IR and ^{31}P and ^{13}C NMR spectroscopy and to assist in identifying the specific site of ligand dissociation in this series of clusters.

Introduction

As part of an extensive agenda to evaluate reaction pathways of polynuclear metal carbonyl derivatives, we have investigated ligand substitutional processes in tetranuclear group 9 metal species. Mechanistic aspects of carbon monoxide displacement reactions in $Co_4(CO)_{12}$ and its phosphine/phosphite derivatives have received much of our attention.[2] For example, the rates of CO dissociation in the sequential CO substitution reactions (eq 1) differed by less than 1 order of magnitude for all complexes

$$Co_4(CO)_{12} \xrightarrow[+L]{-CO} Co_4(CO)_{11}L \xrightarrow[+L]{-CO} Co_4(CO)_{10}L_2 \xrightarrow[+L]{-CO} Co_4(CO)_9L_3 \xrightarrow[+L]{-CO} Co_4(CO)_8L_4 \quad (1)$$

thus far examined. Furthermore, via ligand isotope double-labeling studies we were able to conclusively demonstrate that during ligand substitution reactions of $Co_4(CO)_{12}$ with phosphorus ligands to afford $Co_4(CO)_{11}L$ derivatives *no* cluster fragmentation occurs.[3]

Since ligand substitution processes involving metal carbonyls are often dependent on the nature and concentration of the incoming ligand (L) (eq 2),[4] rate parameters for the individual steps in eq 1 have been determined by employing ^{13}CO as incoming ligand. In this instance because of the low nucleophilicity of

$$\text{rate} = k_{obsd}[M_n(CO)_m] = (k_1 + k_2[L])[M_n(CO)_m] \quad (2)$$

carbon monoxide no ligand-dependent term ($k_2[L]$) is noted in the rate expression. Nevertheless, the ligand-independent pathway may be ascribed to either metal–metal bond fission or M–CO bond dissociation, assuming incoming ligand (L) trapping of the intermediate is fast relative to metal–metal bond re-formation. In efforts to assess the importance of metal–metal bond fission during ligand substitution reactions, where M–M bond cleavage does not lead to cluster fragmentation, rate data for CO displacement in $Co_4(CO)_9$(tripod) have been obtained.[5] In this derivative, which was initially synthesized by Osborn and co-workers,[6] one triangular

(1) (a) Texas A&M University. (b) University of Delaware.

(2) (a) Darensbourg, D. J.; Incorvia, M. J. *J. Organomet. Chem.* **1979**, *171*, 89. (b) Darensbourg, D. J.; Incorvia, M. J. *Inorg. Chem.* **1980**, *19*, 2585. (c) Darensbourg, D. J.; Incorvia, M. J. *Inorg. Chem.* **1981**, *20*, 1911. (d) Darensbourg, D. J.; Peterson, B. S.; Schmidt, R. E., Jr. *Organometallics* **1982**, *1*, 306.

(3) Darensbourg, D. J.; Zalewski, D. J. *Inorg. Chem.* **1984**, *23*, 4382.

(4) Darensbourg, D. J. *Adv. Organomet. Chem.* **1982**, *21*, 113.

(5) Darensbourg, D. J.; Zalewski, D. J.; Delord, T. *Organometallics* **1984**, *3*, 1210.

0020-1669/86/1325-3281$01.50/0

Table I. Crystal and Data Collection Parameters for I–III

formula	$C_{48}Co_4H_{40}O_8P_4{\cdot}CH_2Cl_2$ (I)	$C_{69}Co_4H_{53}O_7P_5{\cdot}2CH_3CN$ (II)	$C_{50}Co_4H_{49}O_7P_5$ (III)
cryst syst	orthorhombic	monoclinic	orthorhombic
space group	*Pbca*	$P2_1/c$	$Pca2_1$
a, Å	16.864 (5)	12.001 (4)	24.831 (6)
b, Å	16.989 (3)	21.955 (10)	11.999 (2)
c, Å	34.676 (9)	25.329 (9)	19.191 (4)
β, deg	90	99.40 (3)	90
V, Å^3	9934.9 (40)	6584.4 (44)	5717.87
Z	8	4	4
ρ(calcd), g cm^{-3}	1.59	1.41	1.34
temp, °C	22	23	22
cryst dimens, mm	0.21 × 0.21 × 0.40	0.40 × 0.36 × 0.38	0.26 × 0.28 × 0.39
radiation (λ, Å)		graphite-monochromated Mo Kα (0.71073)	
diffractometer		Nicolet R3	
abs coeff, cm^{-1}	15.97	11.61	13.19
scan speed, deg min^{-1}	5–20	6–20	5–20
2θ scan range, deg	4–42	4–45	4–45
scan technique	Wyckoff	Wyckoff	Wyckoff
data collcd	$+h,+k,+l$	$+h,+k,+l$	$+h,+k,+l$
no. of unique data	5695	8536	3566
no. of unique data, $F_o \geq n\sigma(F_o)$	2881 (n = 5)	5889 (n = 4)	2840 (n = 3)
no. of std reflcns	3/97 (no decay)	3/197 (no decay)	3/197 (no decay)
R_F, R_{wF}, GOF	0.0626, 0.0589, 1.303	0.0900, 0.0910, 1.679	0.0706, 0.0663, 1.501
highest peak, final diff map, e Å^{-3}	0.71 (in disordered solvent molecule)	1.552 (in disordered solvent molecule)	0.69 (in Co_4 tetrahedron)

Co_3 face is rigidly held in place by the capping tridentate phosphine ligand, greatly retarding metal–metal bond fission.

Reactions of $Co_4(CO)_9$(tripod) with phosphine ligands were undertaken to (i) obtain more highly substituted clusters, (ii) learn more about the specific site(s) for CO dissociation, and (iii) prepare a derivative where stereoselective loss of CO is noted.[7] With regard to the latter objective it was particularly gratifying to obtain the $Co_4(CO)_7$(tripod)(dppm) (dppm = bis(diphenylphosphino)methane) derivative, where stereoselective dissociation of apical CO ligands was observed (eq 3). Comparative rate data

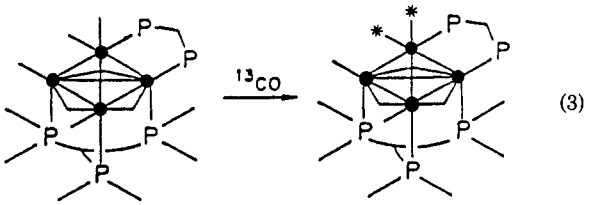

(3)

for CO dissociation in $Co_4(CO)_7$(tripod)(dppm) and $Co_4(CO)_9$(tripod) reveal a slight retardation (by a factor of 5) in the rate of CO dissociation upon substitution of a cobalt center by a phosphine ligand. The activation parameters for dissociative CO loss in the two derivatives were ΔH^* = 24.2 ± 3.3 kcal/mol and ΔS^* = −0.52 ± 10.2 eu for $Co_4(CO)_9$(tripod) and ΔH^* = 24.7 ± 1.0 kcal/mol and ΔS^* = −0.83 ± 3.0 eu for $Co_4(CO)_7$(tripod)(dppm).

The structures of all phosphine substituted $Co_4(CO)_9$(tripod) derivatives were assigned on the basis of solution (^{13}C, ^{31}P) NMR and IR spectroscopy. The herein reported X-ray structural characterization of key complexes in this investigation shows the spectroscopic structural assignments to have been correct in all details.[8]

Experimental Section

All manipulations were performed in a double-manifold Schlenk vacuum line under an atmosphere of dry nitrogen or in an argon-filled drybox. Solvents were dried and deoxygenated by distillation from the appropriate reagent.

Infrared spectra were recorded in 0.10-mm matched NaCl sealed cells on a Perkin-Elmer 283B spectrometer or on an IBM FT-IR Model 85 spectrometer with THF as the solvent. ^{31}P and ^{13}C NMR spectra were recorded on a Varian XL-200 spectrometer. The samples were prepared by dissolving ~100 mg of the cluster complex in 3–5 mL of THF and then filtering this solution through a silica gel column into a 10-mm NMR tube. A 0.10-mL sample of acetone-d_6 was then added for the deuterium lock. Chemical shift values are reported with positive values being downfield. The ^{13}C spectra are referenced to Me_4Si by using the solvent peaks. The ^{31}P spectra were referenced relative to H_3PO_4 by adding a sealed capillary tube containing 85% H_3PO_4 or $P(OCH_3)_3$.

Cluster Synthesis. All three clusters were prepared by previously reported methods.[7] X-ray-quality crystals were grown from a concentrated solution by placing a layer of hexane on top and allowing time for slow diffusion of solvents. The following solvent systems were used: $Co_4(CO)_8(PMe_3)$(tripod) from CH_2Cl_2/hexane; $Co_4(CO)_7$(dppm)(tripod) from CH_3CN/ether/hexane; $Co_4(CO)_7(PMe_3)_2$(tripod) from THF/hexane.

Structure Determination. Crystal data as well as data collection and refinement procedures and parameters are collected in Table I. The unit cell parameters were obtained from the least-squares fit of the angular settings of 25 well-centered reflections (15° < 2θ < 20°). All specimens of I–III examined were of low diffraction quality. All computer programs used are contained in the P3 or SHELXTL (version 4.1) packages of programs distributed by the Nicolet Corp. The intensity data for all structures were corrected for absorption by an empirical ψ-scan technique. In all cases data were collected to a maximum 2θ representing the limits of observed data. Crystals of I were mounted in a capillary tube filled with the mother liquor; II and III were epoxied to glass fibers.

Systematic absences in structures I and II uniquely defined the space groups *Pbca* (orthorhombic) and $P2_1/c$ (monoclinic), respectively. Systematic absences in III were consistent with orthorhombic space groups $Pca2_1$ and *Pcam* (nonstandard setting of *Pbcm*). The noncentrosymmetric alternative $Pca2_1$ was indicated by the statistical distribution of *E* values and confirmed by the rational solution and refinement of the structure.

All structures were solved by using the direct method routine SOLV. The *E* map with the highest combined figures of merit yielded the positions of the Co atoms, and the remaining non-hydrogen atoms were found on subsequent difference Fourier maps. Empirical absorption corrections were applied to the intensity data.

In all cases, final refinement was by blocked-cascade methods using a model containing ellipsoidal thermal parameters for all non-hydrogen atoms except for the phenyl carbon atoms in I and III, which were isotropically refined. Hydrogen atoms were included as idealized, fixed contributions, and phenyl rings were constrained to rigid hexagons. No unusual trends were shown with regard to Miller index, parity group, or sin θ.

For structures I and II partially to severely disordered molecules of solvent (I, CH_2Cl_2; II, CH_3CN) were incorporated as isotropic contributions, but in neither case was it possible to model the disorder completely.

Atomic coordinates for I, II, and III are provided in Tables II, III, and IV, respectively. Selected bond distances and angles are given in Tables V, VI, and VII for structures I, II, and III, respectively. Additional

(6) (a) Arduini, A. A.; Bahsoun, A. A.; Osborn, J. A.; Voelken, C. *Angew. Chem.* **1980**, *92*, 1058; *Angew. Chem., Int. Ed. Engl.* **1980**, *19*, 1024. (b) Osborn, J. A.; Stanley, G. *Angew. Chem., Int. Ed. Engl.* **1980**, *19*, 1025. (c) Bahsoun, A. A.; Osborn, J. A.; Voelken, G.; Bonnet, J. J.; Lavigne, G. *Organometallics* **1982**, *1*, 1114.

(7) Darensbourg, D. J.; Zalewski, D. J. *Organometallics* **1985**, *4*, 92.

(8) During the review of this work[7] a skeptical reviewer wrote "...spectroscopic analysis appears sound but sometimes such analyses are deceptive".

Table II. Atom Coordinates ($\times 10^4$) and Temperature Factors ($Å^2 \times 10^3$) for I[a]

atom	x	y	z	U_{iso}	atom	x	y	z	U_{iso}
Co(1)	5964 (1)	791 (1)	1724 (1)	35 (1)*	C(16)	5285 (4)	2514 (5)	341 (2)	25 (3)
Co(2)	5979 (1)	1881 (1)	1225 (1)	28 (1)*	C(21)	5533 (5)	4262 (5)	538 (2)	47 (4)
Co(3)	5150 (1)	2028 (1)	1806 (1)	27 (1)*	C(22)	5901 (5)	4991 (5)	491 (2)	60 (5)
Co(4)	4766 (1)	1051 (1)	1306 (1)	27 (1)*	C(23)	6562 (5)	5184 (5)	714 (2)	60 (5)
P(1)	5909 (3)	−515 (2)	1716 (1)	48 (2)*	C(24)	6854 (5)	4648 (5)	984 (2)	56 (5)
P(2)	5377 (2)	2747 (2)	855 (1)	28 (1)*	C(25)	6485 (5)	3919 (5)	1031 (2)	37 (4)
P(3)	4472 (2)	3037 (2)	1583 (1)	25 (1)*	C(26)	5825 (5)	3726 (5)	808 (2)	27 (4)
P(4)	3913 (2)	1841 (2)	1018 (1)	24 (1)*	C(31)	3196 (5)	2689 (4)	2062 (2)	22 (3)
O(1a)	7665 (6)	984 (8)	1680 (4)	101 (6)*	C(32)	2492 (5)	2843 (4)	2260 (2)	45 (4)
O(1b)	5993 (7)	776 (7)	2560 (3)	81 (5)*	C(33)	2102 (5)	3559 (4)	2207 (2)	46 (4)
O(2)	3992 (7)	−397 (5)	1072 (3)	69 (5)*	C(34)	2414 (5)	4120 (4)	1956 (2)	41 (4)
O(3)	7555 (6)	2107 (7)	910 (3)	71 (4)*	C(35)	3118 (5)	3966 (4)	1758 (2)	41 (4)
O(4)	4964 (7)	2342 (6)	2618 (3)	79 (5)*	C(36)	3508 (5)	3251 (4)	1811 (2)	27 (3)
O(5)	6699 (6)	2777 (6)	1859 (3)	54 (4)*	C(41)	4750 (5)	4622 (5)	1371 (2)	38 (4)
O(6)	4019 (6)	788 (5)	2050 (3)	45 (4)*	C(42)	5041 (5)	5378 (5)	1438 (2)	40 (4)
O(7)	5955 (6)	459 (5)	755 (3)	51 (4)*	C(43)	5512 (5)	5526 (5)	1760 (2)	51 (4)
Cb	4344 (7)	2868 (7)	1047 (3)	20 (4)*	C(44)	5692 (5)	4917 (5)	2016 (2)	49 (4)
Hb	4041	3269	918	10	C(45)	5400 (5)	4161 (5)	1949 (2)	35 (4)
C(1a)	6976 (10)	922 (9)	1670 (4)	57 (6)*	C(46)	4930 (5)	4013 (5)	1626 (2)	27 (3)
C(1b)	5911 (9)	825 (9)	2229 (4)	46 (6)*	C(51)	2628 (4)	1276 (4)	1422 (2)	26 (3)
C(2)	4296 (8)	173 (8)	1173 (4)	44 (6)*	C(52)	1863 (4)	1278 (4)	1574 (2)	41 (4)
C(3)	6918 (8)	2027 (8)	1034 (4)	39 (5)*	C(53)	1378 (4)	1937 (4)	1528 (2)	47 (4)
C(4)	5041 (8)	2209 (7)	2294 (4)	40 (5)*	C(54)	1659 (4)	2594 (4)	1329 (2)	41 (4)
C(5)	6182 (8)	2439 (8)	1715 (4)	48 (6)*	C(55)	2424 (4)	2592 (4)	1176 (2)	32 (3)
C(6)	4436 (8)	1095 (9)	1827 (4)	37 (6)*	C(56)	2909 (4)	1933 (4)	1222 (2)	25 (3)
C(7)	5694 (7)	900 (8)	990 (4)	33 (5)*	C(61)	3015 (5)	1980 (5)	332 (2)	42 (4)
C(8)	6670 (11)	−944 (9)	2001 (5)	89 (9)*	C(62)	2819 (5)	1759 (5)	−44 (2)	48 (4)
C(9)	5990 (11)	−1083 (9)	1277 (4)	73 (7)*	C(63)	3259 (5)	1179 (5)	−232 (2)	60 (5)
C(10)	5030 (10)	−931 (9)	1939 (4)	74 (7)*	C(64)	3895 (5)	820 (5)	−44 (2)	55 (5)
C(11)	5868 (4)	2035 (5)	178 (2)	42 (4)	C(65)	4091 (5)	1040 (5)	331 (2)	37 (4)
C(12)	5866 (4)	1888 (5)	−217 (2)	60 (5)	C(66)	3651 (5)	1620 (5)	519 (2)	25 (3)
C(13)	5281 (4)	2219 (5)	−451 (2)	51 (4)	Cl(1)	1228 (4)	687 (4)	532 (2)	119 (3)*
C(14)	4697 (4)	2698 (5)	−288 (2)	48 (4)	Cl(2)	2042 (4)	−791 (4)	410 (2)	131 (3)*
C(15)	4700 (4)	2846 (5)	107 (2)	36 (4)	Cs	2106 (11)	184 (7)	525 (8)	135 (12)*

[a] An asterisk indicates the equivalent isotropic U is defined as one-third of the trace of the orthogonalized U_{ij} tensor.

crystallographic data are available as supplementary data.

Results and Discussion

The structures of $Co_4(CO)_8(PMe_3)(HC(PPh_2)_3)$ (I), $Co_4(CO)_7(H_2C(PPh_2)_3)(HC(PPh_2)_3)$ (II), and $Co_4(CO)_7(PMe_3)_2(HC(PPh_2)_3)$ (III) may be discussed in context with the reported structures of other tetrahedral cobalt clusters, in particular those structures containing the face-capping $HC(PPh_2)_3$ moiety. The basic architecture of the above clusters is derived from that of $Co_4(CO)_{12}$ by substituting phosphine ligands for carbonyl groups. In $Co_4(CO)_{12}$ the twelve CO groups form a distorted icosahedron around the tetrahedral core of cobalt atoms.[9] This ligand arrangement provides four unique sets of carbonyl ligands (bridging, axial, equatorial, and apical) and dictates two distinct types of cobalt atoms (apical and basal). In the tripod substituted clusters, the $HC(PPh_2)_3$ ligand replaces the three axial CO groups of the parent cluster. Compounds I–III crystallize as discrete molecular complexes without significant intermolecular contacts.

Structure of $Co_4(CO)_8(PMe_3)(HC(PPh_2)_3)$. Figure 1 presents the molecular geometry and labeling scheme for I. As anticipated from spectroscopic results, the PMe_3 ligand occupies an apical position in the cluster. On substituting $Co_4(CO)_9$(tripod) with PMe_3 the average apical cobalt–carbonyl bond length decreases from 1.793 to 1.743 Å. This shortening is a result of the increased electron density placed on the apical cobalt atom by the strong donor ligand, PMe_3. Some of this added electron density is passed onto the apical carbonyl groups by increasing the amount of π-back-donation. This type of synergistic effect is common in mononuclear organometallic complexes. An added feature that polynuclear metal carbonyl complexes possess is that electronic perturbations occurring at one metal atom can be transmitted to the remaining metal centers of the complex. This communication between metal centers can appear as distortions in the metal–metal bond length or as perturbations in the metal–ligand bond of the cluster.

The mean equatorial metal–carbonyl bond length in $Co_4(CO)_8(PMe_3)$(tripod) (1.737 Å) is slightly shorter than that of $Co_4(CO)_9$(tripod) (1.752 Å). Even though this bond contraction is predicted on the basis of electronic arguments and backed by a shift to lower frequency in the IR spectra, the difference in the bond lengths of the two complexes is less than 3σ and may not be significant.

It is important to note that the bond distances of the apical carbonyls are not significantly different from those of the equatorial carbonyls. Assuming that the bond length is a measure of bond strength, the above observation implies that it is equally likely to dissociate a basal carbonyl group as it is to dissociate an apical group. In previous structures the equatorial Co–CO bond length is shorter than the apical bond length by an average distance of 0.047 Å, suggesting that the apical carbonyl groups will dissociate preferentially.

The three bridging carbonyl groups and the capping tripod ligand work to hold the three basal cobalt atoms in place. Therefore, the basal Co–Co bond distances were not expected to vary substantially upon substitution. Indeed, this is what is observed; in I the basal bond lengths range from 2.466 to 2.500 Å whereas previously reported values vary from 2.438 to 2.491 Å. Earlier we noted that the basal–apical bond distances (2.528–2.590 Å) of tetranuclear cobalt clusters were substantially reduced when the apical carbonyl groups were replaced by an η^6-arene ligand (2.472–2.471 Å).[5] We anticipated a similar shortening upon apical substitution by strong donor ligands such as PMe_3 as was observed in the arene derivatives.[10,11] This phenomenon was not observed

(9) (a) Wei, C. H.; Dahl, L. F. *J. Am. Chem. Soc.* **1966**, *88*, 1812. (b) Wei, C. H.; Wilkes, G. R.; Dahl, L. F. *J. Am. Chem. Soc.* **1967**, *89*, 4792. (c) Wei, C. H. *Inorg. Chem.* **1969**, *8*, 2384. (d) Carre, F. H.; Cotton, F. A.; Frena, B. *Inorg. Chem.* **1976**, *15*, 380.

(10) (a) Khand, I. U.; Knox, G. R.; Pausen, P. L.; Watts, W. E. *Chem. Commun.* **1971**, 36. (b) Khand, I. U.; Knox, G. R.; Pausen, P. L.; Watts, W. E. *J. Chem. Soc., Perkin Trans. 1* **1973**, 975. (c) Bird, P. H.; Fraser, A. R. *J. Organomet. Chem.* **1974**, *73*, 103.

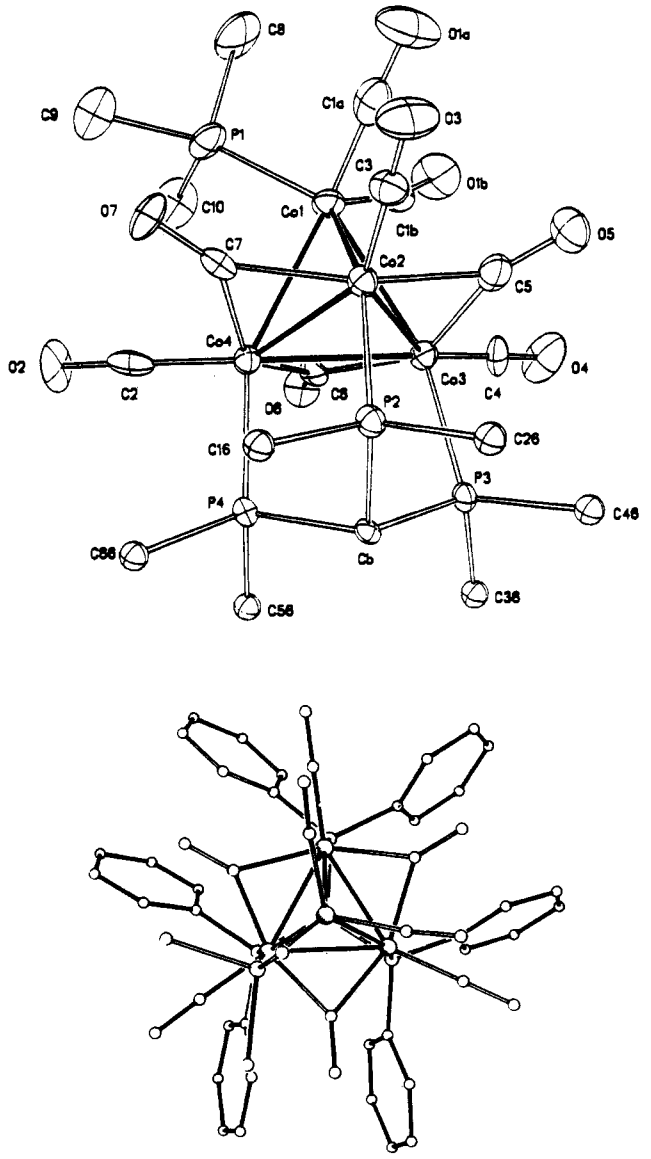

Figure 1. Molecular structure and labeling scheme for I. Only the ipso carbons are shown for the six phenyl rings of the tripod ligand. Thermal ellipsoids are shown at the 40% probability level.

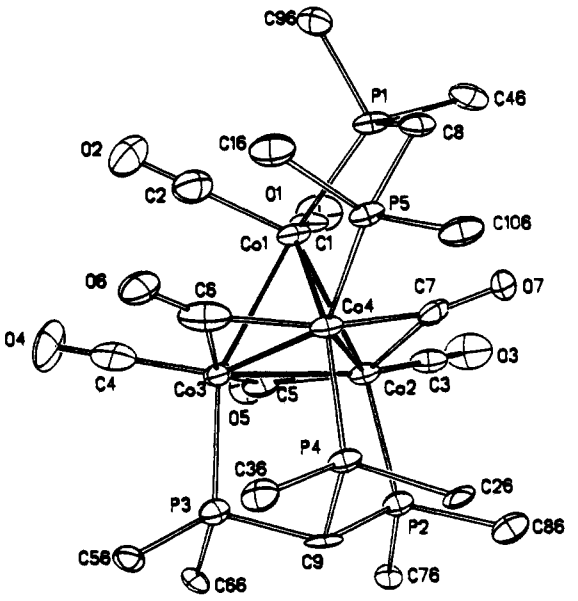

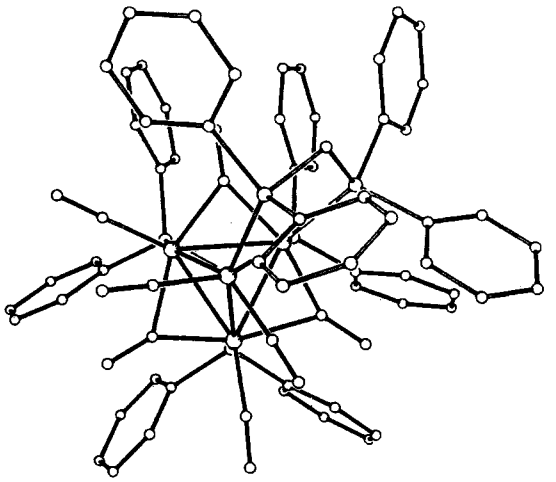

Figure 2. Molecular structure and labeling scheme for II. Only the ipso carbon atoms are shown for the six phenyl rings of the tripod and dppm ligands. Thermal ellipsoids are shown at the 40% probability level.

in I, where the basal–apical distance ranges from 2.524 to 2.535 Å, which is almost identical with that found in $Co_4(CO)_9$tripod (2.529–2.546 Å). The average distance is 0.011 Å shorter in the substituted cluster. A further shortening of this bond might have been prevented by having the apical cobalt atom transfer its extra electron density into the metal–carbonyl bonds instead of the metal–metal bonds.

The bonds from the tripod ligand to the cobalt atoms range from 2.199 to 2.206 Å. These distances are similar to that of $Co_4(CO)_9$(tripod). No unusual bond angles are noted for the tripod ligand. As seen for $Co_4(CO)_9$(tripod), a slight asymmetry exists in the Co_3P_3 trigonal-prismatic unit where each phosphorus atom has two slightly different P–Co–Co angles averaging to 94.4 and 98.3°.

The apical ligands are located directly above the equatorial ligands (Figure 1). Steric considerations favor a position located between the equatorial and bridging groups. This would represent a 30° rotation of the apical ligands from the observed location. This observation, along with the formation of $Co_4(CO)_8(P(n\text{-}Bu)_3)$(tripod), indicates that there are few steric requirements imposed on the apical ligands. The cone angle of PMe_3 (118°) is larger than that of CO (~95°) and does cause some minor perturbations in the cluster.[12] The basal carbonyl ligands located below the PMe_3 ligand are forced down toward the plane formed by the three basal cobalt atoms. The Co(apical)–Co(basal)–CO(equatorial) bond angles are 111.3, 111.9, and 108.4°. Analogous bond angles in $Co_4(CO)_9$(tripod) average to 107.3°.

Structure of $Co_4(CO)_7$(dppm)(tripod). The molecular structure and labeling scheme of II is depicted in Figure 2. The general features of this cluster are identical with that of $Co_4(CO)_9$(tripod) with the dppm ligand bridging between the apical and basal cobalt atoms. The dppm ligand forces the apical groups to rotate slightly from the ideal position. In II the apical ligands are located between the bridging and terminal ligand of the basal plane.

The metal–metal bonds of II are typical for tetrahedral clusters of this type with the average basal–basal and basal–apical bond lengths being 2.460 and 2.541 Å, respectively. The bond bridged by the dppm ligand (2.531 Å) is not substantially different from the unsupported basal–apical bonds.

The apical cobalt contains one long (1.803 (15) Å) and one short (1.758 (12) Å) metal–carbonyl bond. The longer distance

(11) Gancarz, R. A.; Blount, J. F.; Mislow, K. *Organometallics* **1985**, *4*, 2028.

(12) Tolman, C. A. *Chem. Rev.* **1977**, *77*, 313.

Table III. Atomic Coordinates ($\times 10^4$) and Equivalent Isotropic Temperature Factors ($Å^2 \times 10^3$) for II[a]

atom	x	y	z	U_{iso}	atom	x	y	z	U_{iso}
Co(1)	6872 (1)	4286 (1)	2889 (1)	32 (1)*	C(44)	5990 (7)	6660 (4)	3907 (3)	57 (6)
Co(2)	7249 (1)	4643 (1)	1987 (1)	28 (1)*	C(45)	6457 (7)	6076 (4)	3947 (3)	48 (5)
Co(3)	7717 (1)	3591 (1)	2241 (1)	29 (1)*	C(46)	6349 (7)	5701 (4)	3497 (3)	41 (5)
Co(4)	8869 (1)	4413 (1)	2705 (1)	27 (1)*	C(51)	10432 (6)	2719 (3)	1266 (2)	39 (4)
P(1)	7083 (2)	4952 (2)	3563 (1)	34 (1)*	C(52)	11261 (6)	2268 (3)	1327 (2)	40 (4)
P(2)	8244 (2)	4732 (1)	1339 (1)	29 (1)*	C(53)	11488 (6)	1937 (3)	1803 (2)	47 (5)
P(3)	8717 (2)	3430 (1)	1596 (1)	31 (1)*	C(54)	10885 (6)	2058 (3)	2218 (2)	39 (5)
P(4)	10203 (2)	4392 (1)	2186 (1)	27 (1)*	C(55)	10056 (6)	2509 (3)	2157 (2)	36 (4)
P(5)	9632 (2)	4781 (1)	3499 (1)	29 (1)*	C(56)	9829 (6)	2840 (3)	1681 (2)	30 (4)
C(1)	5427 (10)	4412 (6)	2659 (5)	42 (5)*	C(61)	7014 (6)	2797 (4)	957 (2)	38 (4)
O(1)	4474 (7)	4506 (5)	2523 (4)	67 (4)*	C(62)	6509 (6)	2492 (4)	496 (2)	49 (5)
C(2)	6775 (11)	3609 (7)	3282 (6)	53 (5)*	C(63)	6931 (6)	2567 (4)	19 (2)	60 (6)
O(2)	6677 (9)	3188 (5)	3522 (5)	83 (5)*	C(64)	7856 (6)	2947 (4)	2 (2)	52 (5)
C(3)	6167 (10)	5252 (6)	1747 (5)	39 (5)*	C(65)	8360 (6)	3252 (4)	463 (2)	36 (4)
O(3)	5467 (8)	5491 (5)	1605 (4)	65 (4)*	C(66)	7939 (6)	3177 (4)	940 (2)	32 (4)
C(4)	7257 (10)	2851 (7)	2359 (5)	47 (5)*	C(71)	6392 (6)	4422 (4)	564 (3)	56 (6)
O(4)	6897 (9)	2375 (4)	2416 (4)	76 (5)*	C(72)	5807 (6)	4345 (4)	45 (3)	68 (6)
C(5)	6402 (11)	3865 (6)	1828 (5)	41 (5)*	C(73)	6357 (6)	4437 (4)	−393 (3)	72 (7)
O(5)	5505 (7)	3738 (4)	1602 (4)	48 (3)*	C(74)	7493 (6)	4606 (4)	−312 (3)	61 (6)
C(6)	8948 (9)	3601 (7)	2901 (5)	48 (5)*	C(75)	8078 (6)	4684 (4)	207 (3)	44 (5)
O(6)	9291 (7)	3212 (4)	3207 (3)	48 (3)*	C(76)	7528 (6)	4692 (4)	645 (3)	32 (4)
C(7)	8134 (9)	5175 (6)	2523 (4)	31 (4)*	C(81)	8286 (6)	5996 (4)	1373 (3)	45 (5)
O(7)	8116 (6)	5689 (3)	2621 (3)	32 (3)*	C(82)	8645 (6)	6577 (4)	1255 (3)	58 (6)
C(8)	8553 (8)	5223 (5)	3771 (4)	33 (4)*	C(83)	9574 (6)	6646 (4)	993 (3)	64 (6)
C(9)	9444 (9)	4167 (5)	1498 (4)	33 (4)*	C(84)	10144 (6)	6133 (4)	850 (3)	48 (5)
C(11)	9299 (5)	3896 (4)	4242 (4)	51 (5)	C(85)	9785 (6)	5552 (4)	969 (3)	43 (5)
C(12)	9619 (5)	3460 (4)	4637 (4)	72 (7)	C(86)	8856 (6)	5483 (4)	1230 (3)	37 (4)
C(13)	10760 (5)	3365 (4)	4836 (4)	83 (7)	C(91)	5497 (6)	4414 (5)	4086 (3)	61 (6)
C(14)	11581 (5)	3707 (4)	4638 (4)	87 (8)	C(92)	5044 (6)	4196 (5)	4524 (3)	84 (8)
C(15)	11261 (5)	4143 (4)	4242 (4)	57 (5)	C(93)	5671 (6)	4234 (5)	5037 (3)	73 (7)
C(16)	10120 (5)	4238 (4)	4044 (4)	43 (5)	C(94)	6750 (6)	4489 (5)	5114 (3)	88 (8)
C(21)	10669 (5)	5643 (3)	2245 (3)	36 (4)	C(95)	7202 (6)	4707 (5)	4676 (3)	57 (5)
C(22)	11289 (5)	6169 (3)	2188 (3)	43 (5)	C(96)	6575 (6)	4669 (5)	4163 (3)	42 (5)
C(23)	12277 (5)	6135 (3)	1966 (3)	50 (5)	C(101)	10710 (5)	5917 (4)	3759 (3)	47 (5)
C(24)	12646 (5)	5574 (3)	1802 (3)	45 (5)	C(102)	11593 (5)	6333 (4)	3774 (3)	53 (5)
C(25)	12026 (5)	5048 (3)	1859 (3)	31 (4)	C(103)	12582 (5)	6163 (4)	3591 (3)	57 (6)
C(26)	11037 (5)	5082 (3)	2081 (3)	26 (4)	C(104)	12689 (5)	5577 (4)	3391 (3)	53 (6)
C(31)	12017 (6)	3629 (4)	1987 (2)	41 (5)	C(105)	11806 (5)	5161 (4)	3376 (3)	39 (4)
C(32)	12971 (6)	3272 (4)	2154 (2)	47 (5)	C(106)	10816 (5)	5331 (4)	3560 (3)	34 (4)
C(33)	13262 (6)	3111 (4)	2692 (2)	63 (6)	SN(1)[b]	6154 (21)	7548 (12)	448 (11)	184 (10)
C(34)	12598 (6)	3308 (4)	3063 (2)	61 (6)	SC(1)	5764 (20)	7272 (11)	801 (11)	133 (8)
C(35)	11644 (6)	3665 (4)	2896 (2)	40 (4)	SC(2)	5196 (21)	6979 (13)	1170 (12)	155 (10)
C(36)	11354 (6)	3826 (4)	2358 (2)	33 (4)	SN(2)	1138 (14)	4024 (7)	511 (7)	105 (5)
C(41)	5774 (7)	5909 (4)	3007 (3)	46 (5)	SC(3)	1979 (19)	3857 (10)	455 (9)	108 (7)
C(42)	5307 (7)	6493 (4)	2967 (3)	52 (5)	SC(4)	3111 (28)	3570 (15)	391 (15)	209 (14)
C(43)	5415 (7)	6868 (4)	3417 (3)	57 (6)					

[a] An asterisk indicates the equivalent isotropic U is defined as one-third of the trace of the orthogonalized U_{ij} tensor. [b] S atoms = solvent (CH_3CN).

is comparable to the mean apical cobalt–carbonyl bond length of 1.793 Å observed in $Co_4(CO)_9$(tripod). While the shorter distance approaches the average value of 1.743 Å seen for the apical carbonyls in $Co_4(CO)_8(PMe_3)$(tripod). This inequality in bond lengths can be explained by a trans influence. The apical CO groups of $Co_4(CO)_7$(dppm)(tripod) are oriented in such a way that one of the basal cobalt atoms is located nearly trans to the carbonyl group. The carbonyl–Co(apical)–Co(basal) bond angles are 146.5 (4) and 142.5 (4)° for the short and long carbonyls, respectively. The long carbonyl group is trans to a cobalt atom bearing only one phosphine ligand of the tripod moiety. The short carbonyl group has the cobalt atom coordinated to two phosphine ligands trans to it. This substantiates the claim that electronic information can be passed along the metal–metal bonds of a cluster. The observation that the metal–carbonyl bonds in I are slightly shorter than those in II is consistent with the stronger donor ability of the PMe_3 ligand compared to that of $H_2C(PPh_2)_2$.[13] The two equatorial Co–carbonyl bond lengths in II are nearly identical, with values of 1.746 (12) and 1.757 (15) Å. The longest terminal Co–carbonyl distance (1.803 (15) Å) is that of the apical CO ligand. Therefore, if a terminal CO is to dissociate from the cluster, it should dissociate from the apical position. It has been demonstrated earlier that the apical carbonyls of $Co_4(CO)_7$(dppm)(tripod) dissociate preferentially over the equatorial carbonyls.[7]

The bonds to the tripod ligand are unsymmetrical, with the bond to the cobalt atom bearing the dppm ligand being a bit longer than the remaining Co–P bonds (2.208 (4), 2.191 (3), and 2.232 (3) Å). This lengthening is expected on the basis of electronic arguments. The Co–P bond is expected to weaken as the electron density on the cobalt is increased. Steric repulsion between the phenyl groups of the two phosphorus ligands could also explain the lengthening of this bond. However, since the tripod ligand is constructed in such a way as to have a small effective cone angle, steric influences are expected to be minor.

The bonds to the dppm ligand are 2.230 (3) and 2.222 (3) Å, with the apical bond length being the longer of the two. Although this difference is less than 3σ, it follows the trend of this tetrahedral cluster series where the apical bonds are intrinsically weaker than the basal bonds. These bond lengths also provide evidence for the lack of steric repulsion between the tripod and dppm ligands, since the crowded basal site contains a shorter bond than the unhindered apical site.

(13) (a) Dobson, G. R.; Smith, L. A. H. *Inorg. Chem.* **1970**, *9*, 1001. (b) Wovkulich, M. J.; Atwood, J. O. *J. Organomet. Chem.* **1979**, *184*, 77. (c) Cotton, F. A.; Darensbourg, D. J.; Ilsley, W. H. *Inorg. Chem.* **1981**, *20*, 578.

Table IV. Atomic Coordinates ($\times 10^4$) and Equivalent Isotropic Temperature Factors ($Å^2 \times 10^3$) for III[a]

atom	x	y	z	U_{iso}	atom	x	y	z	U_{iso}
Co(1)	3863 (1)	6827 (2)	2075 (1)	54 (1)*	C(14)	4152 (5)	1980 (10)	−712 (4)	58 (6)
Co(2)	3770 (1)	6496 (2)	777 (1)	37 (1)*	C(15)	4396 (5)	2966 (10)	−491 (4)	46 (5)
Co(3)	4636 (1)	7225 (2)	1197 (1)	41 (1)*	C(16)	4357 (5)	3295 (10)	204 (4)	37 (4)
Co(4)	4368 (1)	5299 (2)	1459 (0)	40 (1)*	C(21)	5587 (5)	3041 (10)	167 (5)	57 (6)
P(1)	4724 (2)	4455 (4)	572 (2)	38 (2)*	C(22)	6059 (5)	2442 (10)	288 (5)	84 (7)
P(2)	4055 (2)	6050 (4)	−248 (2)	35 (2)*	C(23)	6333 (5)	2561 (10)	918 (5)	82 (7)
P(3)	5139 (2)	6759 (4)	297 (2)	38 (2)*	C(24)	6135 (5)	3280 (10)	1428 (5)	81 (6)
P(4)	5028 (3)	8761 (5)	1629 (3)	68 (2)*	C(25)	5662 (5)	3879 (10)	1308 (5)	59 (6)
P(5)	3151 (2)	6091 (5)	2652 (3)	63 (2)*	C(26)	5388 (5)	3760 (10)	678 (5)	41 (5)
C(1)	3584 (15)	8193 (23)	2132 (15)	152 (16)*	C(31)	3241 (5)	4481 (10)	−464 (5)	53 (5)
O(1)	3439 (16)	9014 (19)	2207 (16)	272 (19)*	C(32)	2941 (5)	3714 (10)	−848 (5)	61 (6)
C(2)	4232 (9)	6701 (31)	2851 (10)	140 (16)*	C(33)	3088 (5)	3463 (10)	−1532 (5)	60 (6)
O(2)	4441 (7)	6626 (34)	3364 (8)	240 (19)*	C(34)	3535 (5)	3980 (10)	−1831 (5)	58 (6)
C(3)	3083 (9)	6842 (17)	594 (10)	58 (8)*	C(35)	3835 (5)	4747 (10)	−1447 (5)	50 (5)
O(3)	2662 (6)	7070 (15)	500 (11)	118 (9)*	C(36)	3688 (5)	4998 (10)	−763 (5)	38 (4)
C(4)	4448 (7)	4289 (16)	2136 (10)	56 (7)*	C(41)	3644 (4)	7889 (10)	−894 (5)	51 (5)
O(4)	4492 (6)	3632 (14)	2549 (8)	106 (8)*	C(42)	3569 (4)	8630 (10)	−1445 (5)	62 (6)
C(5)	4069 (7)	8031 (16)	788 (10)	44 (7)*	C(43)	3922 (4)	8618 (10)	−2011 (5)	67 (6)
O(5)	3904 (5)	8886 (11)	640 (8)	59 (5)*	C(44)	4350 (4)	7865 (10)	−2025 (5)	65 (6)
C(6)	4979 (7)	6219 (16)	1864 (9)	51 (7)*	C(45)	4425 (4)	7124 (10)	−1473 (5)	53 (5)
O(6)	5313 (5)	6108 (11)	2265 (6)	63 (5)*	C(46)	4072 (4)	7136 (10)	−908 (5)	34 (4)
C(7)	3633 (7)	5126 (17)	1257 (8)	47 (7)*	C(51)	5667 (5)	7610 (9)	−889 (7)	56 (5)
O(7)	3278 (4)	4441 (9)	1324 (6)	52 (5)*	C(52)	5811 (5)	8469 (9)	−1343 (7)	78 (7)
C(8)	4777 (6)	5539 (14)	−118 (8)	34 (6)*	C(53)	5564 (5)	9509 (9)	−1287 (7)	89 (8)
C(9A)	5630 (14)	9382 (30)	1230 (17)	207 (22)*	C(54)	5173 (5)	9691 (9)	−778 (7)	73 (7)
C(9B)	5306 (9)	8696 (19)	2450 (12)	101 (11)*	C(55)	5029 (5)	8833 (9)	−324 (7)	59 (6)
C(9C)	4631 (10)	9985 (16)	1734 (13)	111 (12)*	C(56)	5276 (5)	7793 (9)	−380 (7)	45 (5)
C(10A)	2501 (8)	6083 (17)	2261 (11)	74 (9)*	C(61)	6107 (5)	6645 (10)	1011 (:6)	61 (6)
C(10B)	3200 (8)	4680 (18)	3013 (11)	78 (9)*	C(62)	6649 (5)	6375 (10)	1102 (6)	77 (7)
C(10C)	2972 (9)	6864 (27)	3432 (12)	114 (13)*	C(63)	6907 (5)	5674 (10)	628 (6)	77 (7)
C(11)	4073 (5)	2639 (10)	679 (4)	46 (5)	C(64)	6623 (5)	5243 (10)	62 (6)	72 (7)
C(12)	3829 (5)	1653 (10)	459 (4)	72 (6)	C(65)	6081 (5)	5513 (10)	−30 (6)	49 (5)
C(13)	3868 (5)	1323 (10)	−237 (4)	77 (7)	C(66)	5823 (5)	6214 (10)	444 (6)	47 (5)

[a] An asterisk indicates the equivalent isotropic U is defined as one-third of the trace of the orthogonalized U_{ij} tensor.

Structure of $Co_4(CO)_7(PMe_3)_2$(tripod). Figure 3 presents the molecular arrangement and numbering scheme of III. One phosphine ligand is located at an apical site, while the other is located in an equatorial position. The geometry of this cluster differs from the previous cobalt–tripod structures in that the apical groups are located above the bridging groups instead of the equatorial ligands. This arrangement allows the two PMe_3 ligands to be on opposite sides of the cluster.

The Co–Co bonds in the basal plane are similar to those of structure I and II with a mean value of 2.454 Å. Two short bonds and one long bond connect the basal and apical cobalt atoms (2.517 (3), 2.535 (4), and 2.598 (4) Å). The long bond is undoubtably caused by the steric requirements of the basal phosphine group. The two short bonds are identical with those in $Co_4(CO)_8(PMe_3)$(tripod) and could be caused by the added electron density placed on the apical cobalt atom by the PMe_3 ligand.

The Co–P(tripod) bond lengths are slightly shorter than those in I and II with the average length being 2.177 Å. As seen in II, the bond to the cobalt atom bearing the PMe_3 ligand is slightly longer (0.024 Å) than the other two. The axial–Co–equatorial bond angles in III are 104.6, 101.1, and 102.1°, the largest angle being to the equatorial PMe_3 ligand. All of these angles are larger than the analogous angles in $Co_4(CO)_9$(tripod), which average to 98.7°. This could be the result of shortening the Co–P(tripod) bond length and is further proof that the tripod ligand possesses a small effective cone angle. $Co_4(CO)_6(\pi\text{-}C_7H_8)$(tripod) possesses Co-P(tripod) bonds that are similar to those in $Co_4(CO)_7(PMe_3)_2$(tripod) with a mean value of 2.188 Å.[6] As was seen for III, this short distance causes the axial–Co–equatorial bond angles to open up to a mean value of 103.2°.

The bond distances to the PMe_3 ligands in the basal and apical positions are 2.243 (6) and 2.266 (6) Å, respectively. These values are in agreement with the previously noted trend in this series, where the apical bonds are weaker than the basal bonds. The apical Co–PMe_3 bond is 0.045 Å longer than the analogous bond seen in I. This lengthening could result from the poor overlap of metal and phosphorus orbitals. That is, the metal orbitals used to bond with the apical ligands are directed above the equatorial positions of the cluster. In agreement with the above argument, the apical Co–CO bond lengths are 1.754 (20) and 1.784 (29) Å. This represents a slight increase in Co–CO bond length over the mean value of 1.743 Å observed in I. This lengthening is seen even though $Co_4(CO)_7(PMe_3)_2$(tripod) is expected to have increased π-back-donation to the carbonyl ligands compared to that of I, on the basis of the increased electron density distributed throughout the cluster. However, due to the large esd's associated with the apical carbonyl groups of III, the above bond distances do not strongly support the above trend.

NMR Results. The ^{31}P and ^{13}C NMR data are summarized in Tables VIII and IX for the cobalt–tripod derivatives presented in this paper. It was necessary to determine these spectra at temperatures below −80 °C in order to overcome the adverse effects caused by the cobalt quadrupole; i.e., at lower temperatures T_1 of ^{59}Co ($I = {}^7/_2$) becomes smaller and the ^{31}P and ^{13}C resonances are effectively decoupled.

The ^{31}P NMR spectrum of $Co_4(CO)_8(PMe_3)$(tripod) contains two resonances in a 3:1 ratio. This pattern is consistent with the solid-state structure of compound I. The signal attributed to the tripod ligand is split into a doublet by the apical PMe_3 group with a coupling constant of 50 Hz. This indicates that the apical ligands are capable of facile intramolecular rotation around the top of the cluster. The apical PMe_3 group produces a broad featureless signal. This signal should be coupled to the three phosphorus atoms of the tripod ligand and appear as a quartet, but the apical position is severely broadened by the cobalt quadrupole even at low temperatures. The ^{13}C NMR spectrum of I displays three carbonyl frequencies in a 3:2:3 ratio, assigned to the bridging, apical, and equatorial carbonyl groups. As was observed in the ^{31}P spectra, the apical signals are considerably broadened by the cobalt quadrupole.

The ^{31}P NMR spectrum of $Co_4(CO)_7$(dppm)(tripod) is considerably more complex than that of $Co_4(CO)_8(PMe_3)$(tripod) (Figures 4 and 5). Since the bis(diphenylphosphino)methane ligand occupies both an apical and an equatorial site in the cluster,

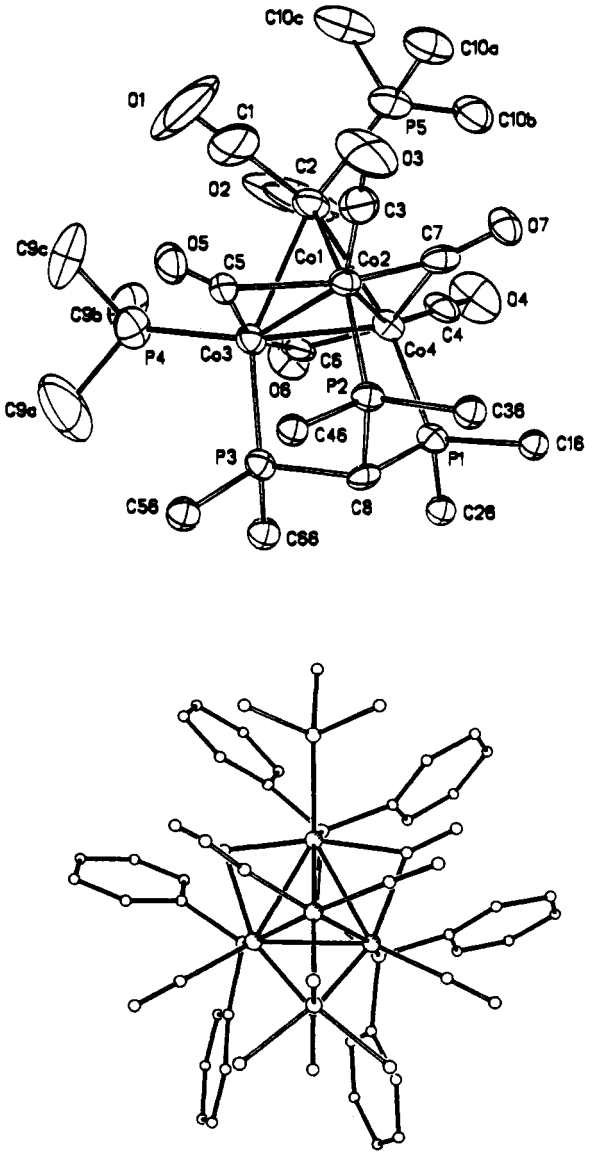

Figure 3. Molecular structure and labeling scheme for III. Only the ipso carbon atoms are shown for the six phenyl rings of the tripod and dppm ligands. Thermal ellipsoids are shown at the 40% probability level.

the C_3 symmetry of the tripod ligand is lost. Therefore, the $HC(PPh_2)_3$ ligand gives rise to two signals in a 1:2 ratio. For simplicity, the labeling scheme

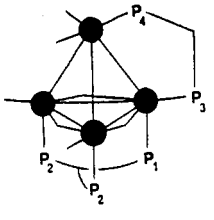

II

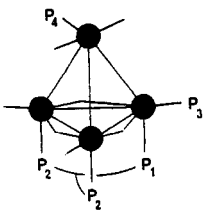

III

will be used to interpret the ^{31}P spectra. The unique phosphorus atom of the tripod ligand (P_1) appears as a triplet ($J_{P_1-P_2}$ = 28 Hz) being coupled to the remaining two phosphorus atoms (P_2) of the tripod ligand. There is no observable coupling of P_1 to the apical or basal phosphine atoms of the dppm ligand. The P_2 atoms appear as a doublet of doublets by virtue of being coupled to both the P_1 atom and the apical P_4 atom ($J_{P_2-P_4}$ = 54 Hz, $J_{P_1-P_2}$ = 28 Hz). The resonance assigned to the P_3 atom appears as a doublet ($J_{P_3-P_4}$ = 55 Hz). This apical–basal coupling occurs through the carbon atom of the ligand and not the metal–metal bond. The apical phosphorus atom (P_4) gives rise to a broad signal as is

Table V. Bond Distances (Å) and Angles (deg) for I

(a) Bond Distances

Co(1)–Co(2)	2.535 (2)	Co(1)–Co(3)	2.528 (3)
Co(1)–Co(4)	2.524 (3)	Co(1)–P(1)	2.221 (4)
Co(1)–C(1a)	1.730 (16)	Co(1)–C(1b)	1.756 (13)
Co(2)–Co(3)	2.466 (2)	Co(2)–Co(4)	2.500 (3)
Co(2)–P(2)	2.199 (4)	Co(2)–C(3)	1.733 (13)
Co(2)–C(5)	1.977 (14)	Co(2)–C(7)	1.917 (14)
Co(3)–Co(4)	2.485 (2)	Co(3)–P(3)	2.200 (4)
Co(3)–C(4)	1.728 (12)	Co(3)–C(5)	1.901 (14)
Co(3)–C(6)	1.992 (15)	Co(4)–P(4)	2.206 (4)
Co(4)–C(2)	1.751 (14)	Co(4)–C(6)	1.891 (14)
Co(4)–C(7)	1.928 (13)	O(1a)–C(1a)	1.168 (20)
O(1b)–C(1b)	1.160 (16)	O(2)–C(2)	1.151 (17)
O(3)–C(3)	1.167 (17)	O(4)–C(4)	1.153 (15)
O(5)–C(5)	1.157 (17)	O(6)–C(6)	1.168 (17)
O(7)–C(7)	1.191 (16)		

(b) Bond Angles

Co(2)–Co(1)–Co(3)	58.3 (1)	Co(2)–Co(1)–P(1)	136.3 (1)
Co(3)–Co(1)–Co(4)	58.9 (1)	Co(4)–Co(1)–P(1)	97.8 (1)
Co(3)–Co(1)–P(1)	144.1 (2)	Co(3)–Co(1)–C(1a)	116.2 (5)
Co(2)–Co(1)–C(1a)	79.8 (5)	P(1)–Co(1)–C(1a)	99.7 (5)
Co(4)–Co(1)–C(1a)	134.8 (5)	Co(3)–Co(1)–C(1b)	80.3 (5)
Co(2)–Co(1)–C(1b)	131.1 (5)	P(1)–Co(1)–C(1b)	92.4 (5)
Co(4)–Co(1)–C(1b)	121.7 (5)	Co(1)–Co(2)–Co(3)	60.7 (1)
C(1a)–Co(1)–C(1b)	98.8 (7)	Co(3)–Co(2)–Co(4)	60.1 (1)
Co(1)–Co(2)–Co(4)	60.2 (1)	Co(3)–Co(2)–P(2)	98.4 (1)
Co(1)–Co(2)–P(2)	151.9 (1)	Co(1)–Co(2)–C(3)	111.9 (5)
Co(4)–Co(2)–P(2)	93.7 (1)	Co(4)–Co(2)–C(3)	150.5 (5)
Co(3)–Co(2)–C(3)	144.6 (4)	Co(1)–Co(2)–C(5)	76.4 (4)
P(2)–Co(2)–C(3)	96.0 (5)	Co(4)–Co(2)–C(5)	108.3 (4)
Co(3)–Co(2)–C(5)	49.2 (4)	C(3)–Co(2)–C(5)	95.8 (6)
P(2)–Co(2)–C(5)	105.1 (4)	Co(3)–Co(2)–C(7)	107.1 (4)
Co(1)–Co(2)–C(7)	69.6 (4)	P(2)–Co(2)–C(7)	102.6 (4)
Co(4)–Co(2)–C(7)	49.6 (4)	C(5)–Co(2)–C(7)	145.7 (6)
C(3)–Co(2)–C(7)	101.0 (6)	Co(1)–Co(3)–Co(4)	60.5 (1)
Co(1)–Co(3)–Co(2)	61.0 (1)	Co(1)–Co(3)–P(3)	153.0 (1)
Co(2)–Co(3)–Co(4)	60.7 (1)	Co(4)–Co(3)–P(3)	98.1 (1)
Co(2)–Co(3)–P(3)	95.0 (1)	Co(2)–Co(3)–C(4)	151.4 (5)
Co(1)–Co(3)–C(4)	108.4 (4)	P(3)–Co(3)–C(4)	98.6 (4)
Co(4)–Co(3)–C(4)	140.6 (4)	Co(2)–Co(3)–C(5)	51.9 (4)
Co(1)–Co(3)–C(5)	77.8 (4)	P(3)–Co(3)–C(5)	97.6 (4)
Co(4)–Co(3)–C(5)	111.6 (4)	Co(1)–Co(3)–C(6)	70.8 (4)
C(4)–Co(3)–C(5)	101.2 (6)	Co(4)–Co(3)–C(6)	48.5 (4)
Co(2)–Co(3)–C(6)	107.0 (4)	C(4)–Co(3)–C(6)	92.4 (6)
P(3)–Co(3)–C(6)	108.6 (4)	Co(1)–Co(4)–Co(2)	60.6 (1)
C(5)–Co(3)–C(6)	148.3 (6)	Co(2)–Co(4)–Co(3)	59.3 (1)
Co(1)–Co(4)–Co(3)	60.6 (1)	Co(2)–Co(4)–P(4)	98.0 (1)
Co(1)–Co(4)–P(4)	152.7 (1)	Co(1)–Co(4)–C(2)	111.3 (5)
Co(3)–Co(4)–P(4)	94.6 (1)	Co(3)–Co(4)–C(2)	150.5 (4)
Co(2)–Co(4)–C(2)	145.2 (4)	Co(1)–Co(4)–C(6)	72.2 (4)
P(4)–Co(4)–C(2)	95.9 (5)	Co(3)–Co(4)–C(6)	52.0 (5)
Co(2)–Co(4)–C(6)	109.1 (5)	C(2)–Co(4)–C(6)	98.7 (6)
P(4)–Co(4)–C(6)	102.5 (5)	Co(2)–Co(4)–C(7)	49.2 (4)
Co(1)–Co(4)–C(7)	69.7 (4)	P(4)–Co(4)–C(7)	110.6 (4)
Co(3)–Co(4)–C(7)	106.0 (4)	C(6)–Co(4)–C(7)	142.0 (6)
C(2)–Co(4)–C(7)	96.0 (6)	Co(1)–P(1)–C(9)	122.6 (5)
Co(1)–C(1a)–O(1a)	171.8 (13)	Co(2)–P(1)–C(10)	114.7 (5)
Co(4)–C(2)–O(2)	177.5 (13)	Co(1)–C(1b)–O(1b)	168.5 (13)
Co(3)–C(4)–O(4)	178.9 (12)	Co(2)–C(3)–O(3)	178.3 (12)
Co(2)–C(5)–O(5)	137.7 (11)	Co(2)–C(5)–Co(3)	78.9 (5)
Co(3)–C(6)–Co(4)	79.5 (5)	Co(3)–C(5)–O(5)	143.2 (12)
Co(2)–Co(1)–Co(4)	59.2 (1)	Co(3)–C(6)–O(6)	138.0 (11)
P(4)–C(6)–P(3)	103.6 (6)	P(4)–C(6)–P(2)	103.7 (6)
P(3)–C(6)–P(2)	105.0 (6)		

typical for clusters in this series. The ^{13}C NMR spectrum possesses the expected four carbonyl signals in a 2:1:2:2 ratio. These are assigned to the two types of bridging carbonyls, the apical carbonyls and the equatorial carbonyls, respectively. As anticipated, the resonances for the two bridging carbon monoxide groups coordinated to the cobalt atom bearing the P_3 atom are located upfield from the remaining μ-CO ligand.

The ^{31}P NMR spectrum of $Co_4(CO)_7(PMe_3)_2$(tripod) exhibits a pattern similar to that of $Co_4(CO)_7$(dppm)(tripod) (Figure 4). The symmetry of the tripod ligand is again disrupted by the basal phosphine ligand. Unlike II, the unique phosphine ligand of III

Table VI. Bond Distances (Å) and Angles (deg) for II

(a) Bond Distances

Co(1)–Co(2)	2.524 (2)	Co(3)–C(5)	1.847 (12)
Co(1)–Co(3)	2.568 (2)	Co(3)–C(4)	1.757 (15)
Co(1)–Co(4)	2.531 (2)	Co(3)–C(6)	2.042 (12)
Co(1)–P(1)	2.230 (3)	Co(4)–P(4)	2.232 (3)
Co(1)–C(1)	1.758 (12)	Co(4)–P(5)	2.222 (3)
Co(1)–C(2)	1.803 (15)	Co(4)–C(6)	1.849 (16)
Co(2)–Co(3)	2.440 (2)	Co(4)–C(7)	1.911 (12)
Co(2)–Co(4)	2.486 (2)	C(1)–O(1)	1.159 (14)
Co(2)–P(2)	2.191 (3)	C(2)–O(2)	1.122 (18)
Co(2)–C(3)	1.746 (12)	C(3)–O(3)	1.136 (16)
Co(2)–C(5)	1.977 (13)	C(4)–O(4)	1.149 (18)
Co(2)–C(7)	1.964 (11)	C(5)–O(5)	1.167 (14)
Co(3)–Co(4)	2.454 (2)	C(6)–O(6)	1.180 (17)
Co(3)–P(3)	2.208 (4)	C(7)–O(7)	1.157 (14)

(b) Bond Angles

Co(2)–C(1)–Co(3)	57.3 (1)	Co(4)–Co(3)–C(5)	113.2 (4)
Co(2)–Co(1)–Co(4)	58.9 (1)	P(3)–Co(3)–C(5)	98.6 (1)
Co(3)–Co(1)–Co(4)	57.5 (1)	C(4)–Co(3)–C(5)	97.7 (6)
Co(2)–Co(1)–P(1)	118.3 (1)	Co(1)–Co(3)–C(6)	77.2 (4)
Co(3)–Co(1)–P(1)	150.6 (1)	Co(2)–Co(3)–C(6)	108.0 (6)
Co(4)–Co(1)–P(1)	94.4 (1)	Co(4)–Co(3)–C(6)	47.5 (4)
Co(2)–Co(1)–C(1)	88.0 (4)	P(3)–Co(3)–C(6)	101.5 (4)
Co(3)–Co(1)–C(1)	110.7 (5)	C(4)–Co(3)–C(6)	94.4 (6)
Co(4)–Co(1)–C(1)	146.5 (4)	C(5)–Co(3)–C(6)	153.9 (6)
P(1)–Co(1)–C(1)	97.6 (4)	Co(1)–Co(4)–Co(2)	60.4 (1)
Co(2)–Co(1)–C(2)	142.5 (5)	Co(1)–Co(4)–Co(3)	62.0 (1)
Co(3)–Co(1)–C(2)	86.0 (5)	Co(2)–Co(4)–Co(3)	59.2 (1)
Co(4)–Co(1)–C(2)	109.9 (4)	Co(1)–Co(4)–P(4)	153.9 (1)
P(1)–Co(1)–C(2)	97.3 (5)	Co(2)–Co(4)–P(4)	97.1 (1)
C(1)–Co(1)–C(2)	99.4 (6)	Co(3)–Co(4)–P(4)	96.0 (1)
Co(1)–Co(2)–Co(3)	62.3 (1)	Co(1)–Co(4)–P(5)	97.8 (1)
Co(1)–Co(2)–Co(4)	60.7 (1)	Co(2)–Co(4)–P(6)	138.2 (1)
Co(3)–Co(2)–Co(4)	59.7 (1)	Co(3)–Co(4)–P(6)	144.8 (1)
Co(1)–Co(2)–P(2)	154.9 (1)	P(4)–Co(4)–P(5)	108.2 (1)
Co(3)–Co(2)–P(2)	98.7 (1)	Co(1)–Co(4)–C(6)	81.5 (4)
Co(4)–Co(2)–P(2)	96.3 (1)	Co(2)–Co(4)–C(6)	113.1 (4)
Co(1)–Co(2)–C(3)	106.3 (4)	Co(3)–Co(4)–C(6)	54.5 (4)
Co(3)–Co(2)–C(3)	145.5 (4)	P(4)–Co(4)–C(6)	97.4 (4)
Co(4)–Co(2)–C(3)	146.4 (4)	P(5)–Co(4)–C(6)	96.4 (4)
P(2)–Co(2)–C(3)	98.5 (4)	Co(1)–Co(4)–C(7)	74.1 (3)
Co(1)–Co(2)–C(5)	75.9 (4)	Co(2)Co(4)–C(7)	51.0 (3)
Co(3)–Co(2)–C(5)	47.9 (3)	Co(3)–Co(4)–C(7)	109.1 (3)
Co(4)–Co(2)–C(5)	106.6 (3)	P(4)–Co(4)–C(7)	102.9 (4)
P(2)–Co(2)–C(5)	104.2 (4)	P(5)–Co(4)–C(7)	90.3 (3)
C(3)–Co(2)–C(5)	98.8 (6)	C(6)–Co(4)–C(7)	166.4 (6)
Co(1)–Co(2)–C(7)	73.5 (4)	Co(1)–C(1)–O(1)	177.8 (12)
Co(3)–Co(2)–C(7)	107.8 (3)	Co(1)–C(2)–O(2)	177.7 (12)
Co(4)–Co(2)–C(7)	49.2 (3)	Co(2)–C(3)–O(3)	178.0 (12)
P(2)–Co(2)–C(7)	99.6 (4)	Co(3)–C(4)–O(4)	175.9 (10)
C(3)–Co(2)–C(7)	98.5 (5)	Co(2)–C(5)–Co(3)	98.7 (5)
C(5)–Co(2)–C(7)	148.1 (6)	Co(2)–C(5)–C(6)	134.6 (10)
Co(1)–Co(3)–Co(2)	60.5 (1)	Co(3)–C(5)–O(5)	146.6 (11)
Co(1)–Co(3)–Co(4)	60.5 (1)	Co(3)–C(6)–Co(4)	78.0 (6)
Co(2)–Co(3)–Co(4)	61.1 (1)	Co(3)–C(6)–O(6)	131.0 (11)
Co(1)–Co(3)–P(3)	152.4 (1)	Co(4)–C(6)–O(6)	150.6 (11)
Co(2)–Co(3)–P(3)	94.9 (2)	Co(2)–C(7)–Co(4)	79.8 (5)
Co(4)–Co(3)–P(3)	98.0 (1)	Co(2)–C(7)–O(7)	134.5 (8)
Co(1)–Co(3)–C(4)	105.9 (4)	Co(4)–C(7)–O(7)	145.7 (8)
Co(2)–Co(3)–C(4)	148.8 (4)	P(1)–C(8)–P(5)	114.9 (6)
Co(4)–Co(3)–C(4)	140.2 (4)	P(2)–C(9)–P(3)	103.8 (5)
P(3)–Co(3)–C(4)	101.7 (4)	P(2)–C(9)–P(4)	105.0 (6)
Co(1)–Co(3)–C(5)	77.2 (4)	P(3)–C(9)–P(4)	105.5 (3)
Co()–Co(3)–C(5)	53.4 (4)		

Table VII. Bond Distances (Å) and Angles (deg) for III

(a) Bond Distances

Co(1)–Co(2)	2.535 (4)	Co(3)–P(4)	2.243 (6)
Co(1)–Co(3)	2.598 (4)	Co(3)–C(5)	1.880 (19)
Co(1)–Co(4)	2.517 (3)	Co(3)–C(6)	1.953 (18)
Co(1)–P(5)	2.266 (6)	Co(4)–P(1)	2.169 (5)
Co(1)–C(1)	1.784 (29)	Co(4)–C(4)	1.783 (20)
Co(1)–C(2)	1.754 (20)	Co(4)–C(6)	2.029 (18)
Co(2)–Co(3)	2.458 (3)	Co(4)–C(7)	1.817 (18)
Co(2)–Co(4)	2.447 (3)	C(1)–O(1)	1.058 (28)
Co(2)–P(2)	2.158 (5)	C(2)–O(2)	1.116 (26)
Co(2)–C(3)	1.789 (23)	C(3)–O(3)	1.097 (28)
Co(2)–C(5)	1.986 (20)	C(4)–O(4)	1.123 (26)
Co(2)–C(7)	1.916 (19)	C(5)–O(5)	1.140 (23)
Co(3)–Co(4)	2.457 (3)	C(6)–O(6)	1.140 (21)
Co(3)–P(3)	2.205 (5)	C(7)–O(7)	1.213 (21)

(b) Bond Angles

Co(2)–Co(1)–Co(3)	57.2 (1)	Co(1)–Co(3)–C(5)	79.2 (6)
Co(2)–Co(1)–Co(4)	57.9 (1)	Co(2)–Co(3)–C(5)	52.5 (6)
Co(3)–Co(1)–Co(4)	57.4 (1)	Co(4)–Co(3)–C(5)	111.5 (6)
Co(2)–Co(1)–P(5)	110.3 (2)	P(3)–Co(3)–C(5)	103.2 (6)
Co(3)–Co(1)–P(5)	164.8 (2)	P(4)–Co(3)–C(5)	93.3 (6)
Co(4)–Co(1)–P(5)	109.6 (2)	Co(1)–Co(3)–C(6)	77.5 (5)
Co(2)–Co(1)–C(1)	99.7 (10)	Co(2)–Co(3)–C(6)	112.1 (5)
Co(3)–Co(1)–C(1)	99.1 (10)	Co(4)–Co(3)–C(6)	53.3 (5)
Co(4)–Co(1)–C(1)	153.1 (10)	P(3)–Co(3)–C(6)	96.3 (5)
P(5)–Co(1)–C(1)	91.4 (11)	P(4)–Co(3)–C(6)	94.4 (6)
Co(2)–Co(1)–C(2)	150.3 (9)	C(3)–Co(3)–C(6)	166.5 (8)
Co(3)–Co(1)–C(2)	100.4 (7)	Co(1)–Co(4)–Co(2)	61.4 (1)
Co(4)–Co(1)–C(2)	94.4 (10)	Co(1)–Co(4)–Co(3)	63.0 (1)
P(5)–Co(1)–C(2)	87.7 (8)	Co(2)–Co(4)–Co(3)	60.2 (1)
C(1)–Co(1)–C(2)	103.3 (15)	Co(1)–Co(4)–P(1)	155.8 (2)
Co(1)–Co(2)–Co(3)	62.7 (1)	Co(2)–Co(4)–P(1)	95.8 (1)
Co(1)–Co(2)–Co(4)	60.7 (1)	Co(3)–Co(4)–P(1)	99.7 (1)
Co(3)–Co(2)–Co(4)	60.1 (1)	Co(1)–Co(4)–C(4)	102.0 (6)
Co(1)–Co(2)–P(2)	154.8 (2)	Co(2)–Co(4)–C(4)	148.7 (5)
Co(3)–Co(2)–P(2)	95.8 (2)	Co(3)–Co(4)–C(4)	139.1 (6)
Co(4)–Co(2)–P(2)	98.2 (1)	P(1)–Co(4)–C(4)	102.1 (6)
Co(1)–Co(2)–C(3)	104.1 (6)	Co(1)–Co(4)–C(6)	78.2 (6)
Co(3)–Co(2)–C(3)	144.6 (6)	Co(2)–Co(4)–C(6)	109.8 (5)
Co(4)–Co(2)–C(3)	145.1 (7)	Co(3)–Co(4)–C(6)	50.5 (6)
P(2)–Co(2)–C(3)	101.1 (7)	P(1)–Co(4)–C(6)	104.5 (6)
Co(1)–Co(2)–C(5)	79.0 (3)	C(4)–Co(4)–C(6)	90.5 (8)
Co(3)–Co(2)–C(5)	48.6 (5)	Co(1)–Co(4)–C(7)	72.1 (6)
Co(4)–Co(2)–C(5)	108.2 (5)	Co(2)–Co(4)–C(7)	50.5 (6)
P(2)–Co(2)–C(5)	96.8 (6)	Co(3)–Co(4)–C(7)	109.0 (6)
C(3)–Co(2)–C(5)	98.2 (8)	P(1)–Co(4)–C(7)	100.5 (5)
Co(1)–Co(2)–C(7)	71.1 (5)	C(4)–Co(4)–C(7)	100.5 (8)
Co(3)–Co(2)–C(7)	107.6 (5)	C(6)–Co(4)–C(7)	149.9 (8)
Co(4)–Co(2)–C(7)	49.1 (5)	Co(4)–P(1)–C(8)	109.1 (5)
C(2)–Co(2)–C(7)	106.5 (5)	Co(1)–C(1)–O(1)	174.8 (34)
C(3)–Co(2)–C(7)	97.2 (8)	Co(1)–C(2)–O(2)	176.2 (24)
C(5)–Co(2)–C(7)	148.9 (7)	Co(2)–C(3)–O(3)	177.9 (21)
Co(1)–Co(3)–Co(2)	60.1 (1)	Co(4)–C(4)–O(4)	178.0 (16)
Co(1)–Co(3)–Co(4)	59.6 (10)	Co(2)–C(5)–Co(3)	78.9 (7)
Co(2)–Co(3)–Co(4)	59.7 (1)	Co(2)–C(5)–O(5)	134.2 (15)
Co(1)–Co(3)–P(3)	151.7 (2)	Co(3)–C(5)–O(5)	146.7 (16)
Co(2)–Co(3)–P(3)	98.5 (2)	Co(3)–C(6)–Co(4)	76.2 (6)
Co(4)–Co(3)–P(3)	94.3 (2)	Co(3)–C(6)–O(6)	146.3 (16)
Co(1)–Co(3)–P(4)	103.4 (2)	Co(4)–C(6)–O(6)	137.6 (15)
Co(2)–Co(2)–P(4)	142.5 (2)	Co(2)–C(7)–Co(4)	80.3 (7)
Co(4)–Co(3)–P(4)	144.6 (2)	Co(2)–C(7)–O(7)	139.6 (14)
P(3)–Co(3)–P(4)	104.6 (2)	Co(4)–C(7)–O(7)	139.5 (15)
P(3)–C(8)–P(1)	105.9 (7)	P(3)–C(8)–P(2)	104.6 (8)
P(2)–C(8)–P(1)	104.6 (8)		

(P_1) is coupled to the apical phosphine atom ($J_{P_1-P_4}$ = 120 Hz). The magnitude of this phosphorus–phosphorus coupling constant is consistent with the trans arrangement of the P_1 and P_4 groups. The P_1 atom is also coupled through the tripod ligand to the P_2 atoms ($J_{P_1-P_2}$ = 31 Hz). This results in the P_1 signal appearing as a doublet of triplets. A coupling constant of only 30 Hz is observed between the apical phosphine and the P_2 atoms of the tripod ligand.[14] The P_2 atoms are also coupled to the P_1 atoms ($J_{P_2-P_1}$ = 31 Hz). The nearly identical coupling constants of 30 and 31 Hz make the doublet of doublets pattern of P_1 appear as a triplet (Figure 4). As in II, the equatorial phosphine ligand (P_3) of III is not coupled to the tripod ligand and its signal appears as a singlet. The apical phosphine signal is broadened, but due to the large coupling constant ($J_{P_1-P_4}$ = 120 Hz) it is resolved into a doublet. The smaller coupling to P_2 cannot be seen. The ^{13}C NMR spectrum of III is nearly identical with that of II in that it contains four carbonyl signals in a 2:1:2:2 ratio. These signals are assigned to the two types of bridging groups, the apical ligands and the equatorial groups, respectively.

(14) The P_4 and P_2 atoms can be considered as occupying cis positions in the cluster.

Table VIII. ^{31}P NMR of Cobalt–tripod Clusters[a]

cluster	phosphorus ligand	shift, ppm	rel intens	multiplicity[c] (J, Hz)
$Co_4(CO)_9(tripod)$[b,6]	$HC(PPh_2)_3$	44.3		br, s
$Co_4(CO)_8(PMe_3)(tripod)$ (I)	$HC(PPh_2)_3$	42.9	3	d (50)
	PMe_3	5.4	1	br
$Co_4(CO)_7(dppm)(tripod)$ (II)	$HC(PPh_2)_3$	45.6	1	t (28)
		44.2	2	dd (54, 28)
	dppm (basal)	24.7	1	d (55)
	dppm (apical)	18.2	1	br
$Co_4(CO)_7(PMe_3)_2(tripod)$ (III-B)	$HC(PPh_2)_3$	26.5	3	t (64)
	PMe_3	2.9	2	br
$Co_4(CO)_7(PMe_3)_2(tripod)$ (III)	$HC(PPh_2)_3$	48.2	1	dt (120, 31)
		45.8	2	dd (31, 30)
	PMe_3 (basal)	−1.2	1	s
	PMe_3 (apical)	−4.2	1	br, d (120)

[a] Spectra were recorded at −80 °C with CH_2Cl_2/benzene-d_6 as the solvent unless otherwise stated. [b] CD_2Cl_2 was used as the solvent. [c] s = singlet, d = doublet, t = triplet, br = broad, dd = doublet of doublets, dt = doublet of triplets.

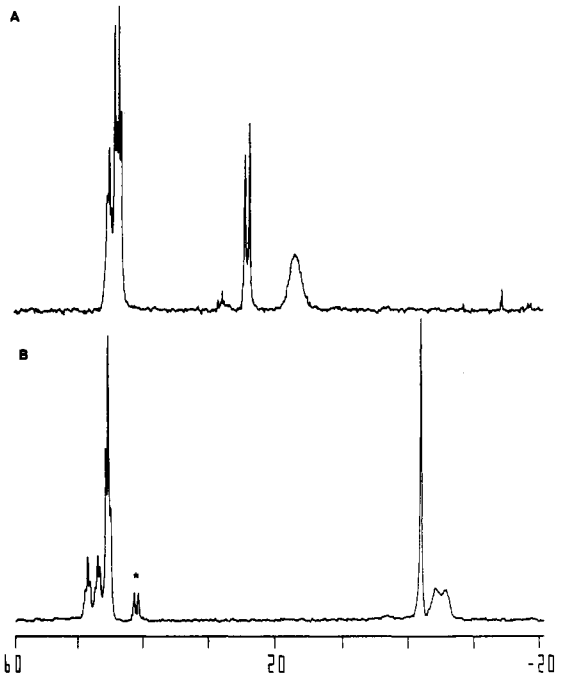

Figure 4. Comparison of the ^{31}P NMR spectra of (A) $Co_4(CO)_7$-(dppm)(tripod) (II) and (B) $Co_4(CO)_7(PMe_3)_2(tripod)$ (III). The spectrum of III shows the presence of a small amount of I (*).

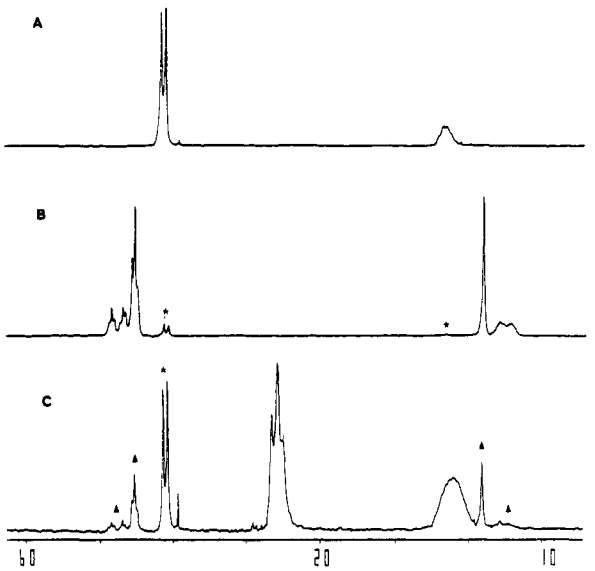

Figure 5. ^{31}P NMR spectra of the trimethylphosphine substituted cobalt–tripod clusters: (A) $Co_4(CO)_8(PMe_3)(tripod)$ (I); (B) $Co_4(CO)_7$-$(PMe_3)_2(tripod)$ (III) (impurity peak assigned to I (*); (C) $Co_4(CO)_7$-$(PMe_3)_2(tripod)$ (III-B) (impurity peaks due to I (*) and III (▲)).

Table IX. ^{13}C NMR Frequency Assignments for the Carbonyl Ligands in Cobalt–tripod Clusters[a]

complex	bridging	apical	equatorial
$Co_4(CO)_9(tripod)$	254.6	203.2	202.0
$Co_4(CO)_8(PMe_3)(tripod)$ (I)	258.1	206.8	203.2
$Co_4(CO)_7(dppm)(tripod)$ (II)	264.1, 257.8	208.3	203.8
$Co_4(CO)_7(PMe_3)_2(tripod)$ (III-B)	263.7	*b*	205.5
$Co_4(CO)_7(PMe_3)_2(tripod)$ (III)	266.8, 266.1	208.3	203.8

[a] Spectra recorded with CD_2Cl_2 as the solvent. The reported frequencies are referenced with the solvent signal and given in ppm downfield from Me_4Si. [b] Peak assigned to the apical position was not observed.

When $Co_4(CO)_8(PMe_3)(tripod)$ is reacted with PMe_3 in THF, the first formed species proved to be too unstable to isolate. On the basis of in situ IR, ^{31}P NMR, and ^{13}C NMR spectra, this cluster is believed to be a bis(trimethylphosphine) substituted cobalt–tripod cluster, III-B, where both of the trimethylphosphine ligands occupy apical sites. III-B rearranges with decomposition to give I and III as products (eq 4).

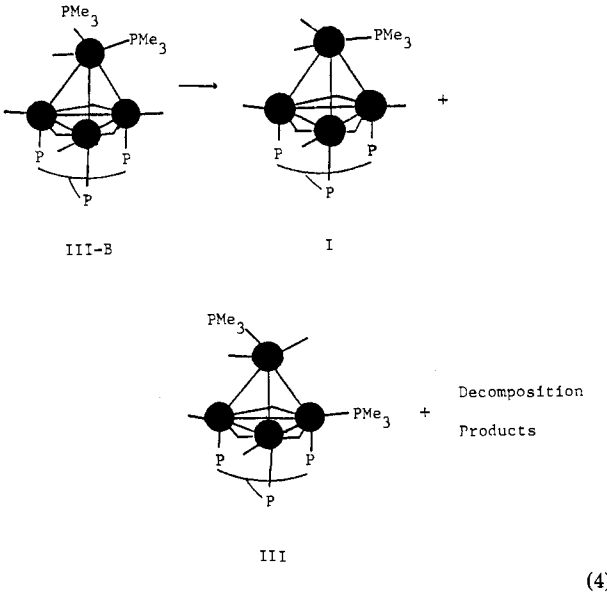

(4)

Refluxing PMe_3 with $Co_4(CO)_8(PMe_3)(tripod)$ in THF for 1 h leads to the formation of III-B. The ^{31}P NMR spectrum contains peaks assigned to unreacted I, III-B, and III, with III-B being the major isomer present (Figure 5). The signal for the tripod ligand of this unstable isomer appears as a triplet (J_{P-P} = 64 Hz), by virtue of it being coupled to the two equivalent apical phosphine ligands. The trimethylphosphine ligands give a very broad signal, as is typical for ligands in the apical positions. The ^{13}C NMR spectrum of III-B is also complicated by the presence of the clusters I and III. Only one bridging carbonyl signal is observed for III-B. This supports the apical location of the PMe_3 groups.

Table X. Comparative Bond Distances (Å) in $Co_4(CO)_{9-n}(L)_n$(tripod) Derivatives

	$Co_4(CO)_9$(tripod)[5]		$Co_4(CO)_8(PMe_3)$(tripod)		$Co_4(CO)_7$(dppm)(tripod)		$Co_4(CO)_7(PMe_3)_2$(tripod)		$Co_4(CO)_6(\pi\text{-}C_7H_8)$(tripod)	
bond type	av	dist	av	dist	av	dist	av	dist	av	dist
Co–Co										
basal–apical	2.540	2.529, 2.546, 2.546	2.529	2.524, 2.535, 2.528	2.541	2.524, 2.568, 2.531	2.550	2.517, 2.598, 2.535	2.472	2.448, 2.490, 2.479
basal–basal	2.457	2.447, 2.467, 2.456	2.484	2.466, 2.500, 2.485	2.460	2.440, 2.486, 2.454	2.454	2.447, 2.458, 2.457	2.447	2.438, 2.456, 2.446
Co–C(br)	1.933	1.904–1.954	1.934	1.891–1.992	1.932	1.847–2.042	1.930	1.817–2.029	1.912	1.89–1.94
Co–C(term)										
apical	1.793	1.784, 1.798, 1.794	1.743	1.730, 1.756	1.780	1.758, 1.803	1.869	1.754, 1.984		
equatorial	1.752	1.738, 1.769, 1.748	1.737	1.728, 1.751, 1.733	1.752	1.746, 1.757	1.786	1.783, 1.789	1.753	1.74, 1.77, 1.75
Co–P										
tripod	2.206	2.203, 2.208, 2.207	2.202	2.199, 2.206, 2.200	2.210	2.191, 2.232, 2.208	2.177	2.158, 2.205, 2.169	2.188	2.174, 2.202, 2.188
apical				2.221		2.230		2.266		
equatorial						2.222		2.243		

Scheme I[a]

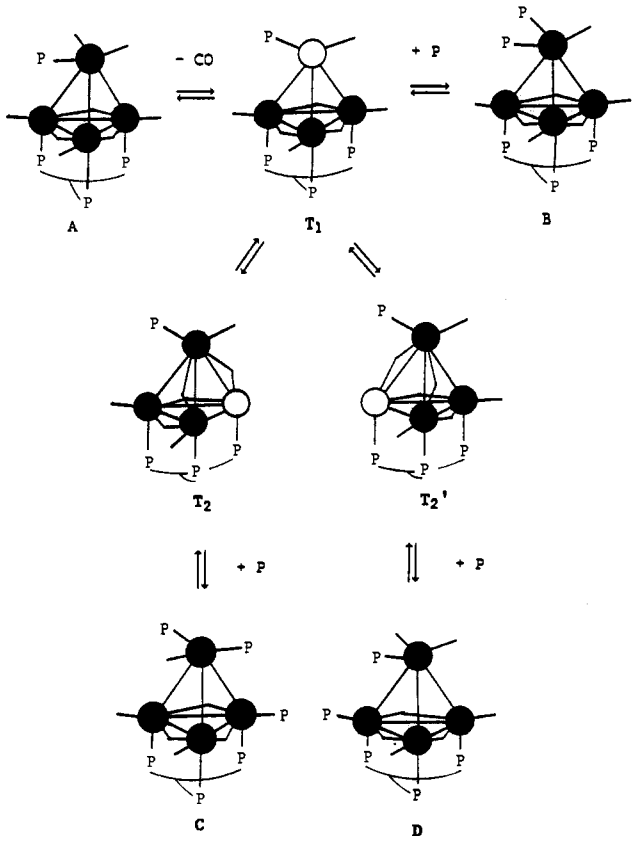

[a] Open circles represent unsaturated metal centers.

Basal substitution would break up the C_3 symmetry of the bridging carbonyls.

Monitoring the reaction by IR spectroscopy shows that the carbonyl frequency of cluster I disappears and the new frequencies of III-B appear at lower frequencies to those of I. With time, peaks assignable to isomer III grow in.

Conclusion

Selected bond distances of the cobalt–tripod clusters are compiled in Table X. This table shows that substituting carbonyl groups with phosphine ligands does not significantly alter the lengths of the metal–metal or metal–ligand bonds. Upon examination of Table X two trends can be noted: (1) the cobalt–cobalt bonds in the basal plane are shorter than those involving apical–basal cobalt atoms, and (2) the apical groups possess longer metal–ligand bonds than identical ligands located at equatorial sites. This latter feature has significance for ligand substitutional processes in this cluster system. Since the apical groups have weaker metal–ligand bonds, these ligands will dissociate preferentially over the equatorial ligands.

When two phosphine ligands are incorporated into the cluster, the steric repulsion between them induces a rotation of the apical groups. This new orientation minimizes the phosphine–phosphine interactions and thereby stabilizes the cluster. However, this rotation also lengthens the metal–ligand bonds of the apical groups. Presumably, this is the result of the poorer molecular orbital overlap associated with this orientation. The orbitals of the apical cobalt atom are directed above the equatorial ligands. It is important to point out that the difference in the ground-state energy associated with either orientation is small. In $Co_4(CO)_8(PMe_3)$(tripod) the apical groups exhibit facile migration about the top of the cluster even at −80 °C.

With the above features in mind, we can rationalize the formation of clusters with the geometry of I, II, III-B, and III (Scheme I) by a carbonyl dissociative process. Dissociation of an apical carbonyl group from the parent cluster $Co_4(CO)_9$(tripod) leads to an intermediate that rapidly adds a phosphine ligand to form the apical substituted cobalt–tripod cluster A. Dissociation of another apical CO group from A forms the unsaturated transition state T_1. T_1 can add a second phosphine ligand to form the unstable cluster B, where both phosphine ligands occupy apical sites. A rearrangement of the carbonyl ligands in T_1 leads to the formation of T_2 or T_2', which have the unsaturated cobalt atom in the basal plane. T_2 and T_2' differ by the location of the apical phosphine atom. The addition of a phosphine ligand to T_2 results in the formation of a cluster containing trans phosphine ligands, C. Adding a phosphine group to T_2' leads to a cis arrangement of the phosphine ligands, D. In T_2, the unsaturated cobalt atom lies below the bulky apical phosphine group. Therefore, it is less likely that incoming ligands would attack this intermediate; it would instead prefer to attack intermediate T_2. Only when the apical phosphine was a bidentate ligand (dppm) was the formation of D observed.

Acknowledgment. The financial support of the Robert A. Welch Foundation is greatly appreciated.

Supplementary Material Available: Listings of bond distances, bond angles, anisotropic temperature factors, and hydrogen atom coordinates for I–III (16 pages); listings of calculated and observed structure factors for I–III (69 pages). Ordering information is given on any current masthead page.